AJNR

Clinical Assessment of Standard and Generalized Autocalibrating Partially Parallel Acquisition Diffusion Imaging: Effects of Reduction Factor and Spatial Resolution

J.B. Andre, G. Zaharchuk, N.J. Fischbein, M. Augustin, S. Skare, M. Straka, J. Rosenberg, M.G. Lansberg, S. Kemp, C.A.C. Wijman, G.W. Albers, N.E. Schwartz and R. Bammer

AJNR Am J Neuroradiol 2012, 33 (7) 1337-1342
doi: https://doi.org/10.3174/ajnr.A2980
http://www.ajnr.org/content/33/7/1337

ORIGINAL RESEARCH

Clinical Assessment of Standard and Generalized Autocalibrating Partially Parallel Acquisition Diffusion Imaging: Effects of Reduction Factor and Spatial Resolution

J.B. Andre
G. Zaharchuk
N.J. Fischbein
M. Augustin
S. Skare
M. Straka
J. Rosenberg
M.G. Lansberg
S. Kemp
C.A.C. Wijman
G.W. Albers
N.E. Schwartz
R. Bammer

BACKGROUND AND PURPOSE: PI improves routine EPI-based DWI by enabling higher spatial resolution and reducing geometric distortion, though it remains unclear which of these is most important. We evaluated the relative contribution of these factors and assessed their ability to increase lesion conspicuity and diagnostic confidence by using a GRAPPA technique.

MATERIALS AND METHODS: Four separate DWI scans were obtained at 1.5T in 48 patients with independent variation of in-plane spatial resolution (1.88 mm^2 versus 1.25 mm^2) and/or reduction factor (R = 1 versus R = 3). A neuroradiologist with access to clinical history and additional imaging sequences provided a reference standard diagnosis for each case. Three blinded neuroradiologists assessed scans for abnormalities and also evaluated multiple imaging-quality metrics by using a 5-point ordinal scale. Logistic regression was used to determine the impact of each factor on subjective image quality and confidence.

RESULTS: Reference standard diagnoses in the patient cohort were acute ischemic stroke (n = 30), ischemic stroke with hemorrhagic conversion (n = 4), intraparenchymal hemorrhage (n = 9), or no acute lesion (n = 5). While readers preferred both a higher reduction factor and a higher spatial resolution, the largest effect was due to an increased reduction factor (odds ratio, 47 ± 16). Small lesions were more confidently discriminated from artifacts on R = 3 images. The diagnosis changed in 5 of 48 scans, always toward the reference standard reading and exclusively for posterior fossa lesions.

CONCLUSIONS: PI improves DWI primarily by reducing geometric distortion rather than by increasing spatial resolution. This outcome leads to a more accurate and confident diagnosis of small lesions.

ABBREVIATIONS: GRAPPA = generalized autocalibrating partially parallel acquisition; PE = phase encode; PI = parallel imaging; R = reduction factor; SS = single-shot

BRAIN

ORIGINAL RESEARCH

DWI has become routine in neuroimaging[1] and is particularly useful for evaluating acute stroke.[2-6] Traditional SS–EPI-based DWI has been most widely used due to its insensitivity to bulk motion and its short acquisition time. The SS–EPI-DWI technique, however, has poor spatial resolution, blurring, and geometric distortion, all of which can compromise diagnosis of small lesions.[7] PI uses spatially separated receiver coils and incomplete sampling of *k*-space, usually accomplished by reducing the number of phase-encoding steps necessary to generate an image.[8,9] While parallel imaging is normally used to shorten overall imaging time, for SS–EPI it results in a faster *k*-space traversal with largely unchanged total imaging time, thus reducing phase errors[9-11] and spatial distortions. These changes can be used to reduce geometric distortions and TE, the latter of which mitigates the signal intensity–to-noise-ratio penalties associated with PI.[12]

If one neglects gradient nonlinearities and Maxwell terms, geometric distortions in SS–EPI are due predominantly to variations in magnetic susceptibility (susceptibility artifacts) that can manifest very locally as signal-intensity pile-up or as geometric distortion. Thus, PI reduces both geometric distortion and susceptibility artifacts (because both are related terms). Alternatively, PI can be used to acquire higher in-plane resolution due to a shortened EPI readout. Higher resolution would be desirable to distinguish small lesions from artifacts. Moreover, acquiring smaller voxels in and of itself leads to reduction in intravoxel dephasing and thus less geometric distortion. For these reasons, we sought to evaluate the relative contributions of each of these factors by using a variant of the GRAPPA technique (see Brau et al[13]).

Materials and Methods

This prospective inter- and intraobserver comparative study was performed at a university stroke center. It was approved by the local

Received September 25, 2011; accepted after revision November 15.

From the Department of Radiology (J.B.A., G.Z., N.J.F., S.S., M.S., J.R., R.B.), Stanford University, Stanford, California; Department of Radiology (M.A.), University of Graz, Graz, Austria; Department of Neurology and Neurological Sciences (M.G.L., S.K., C.A.C.W., G.W.A., N.E.S.), Stanford Stroke Center, Stanford University Medical Center, Stanford California; and Department of Neurology and Neurological Sciences (C.A.C.W.), Stanford Neurocritical Care Program, Stanford Stroke Center, Stanford University Medical Center, Stanford, California.

Paper previously presented in part at: 19th Scientific Meeting of the International Society of Magnetic Resonance in Medicine, May 6–13, 2011; Montreal, Quebec, Canada; and 49th Annual Meeting of the American Society of Neuroradiology and the Neuroradiology Education and Research Foundation Symposium, June 4–9, 2011; Seattle, Washington.

This research was supported by NIH (grant #5R01EB002711).

Please address correspondence to Jalal B. Andre, MD, Department of Radiology, University of Washington, 1959 Pacific St, NM011 Seattle, WA 98195-8475; e-mail: drjalal@uw.edu

http://dx.doi.org/10.3174/ajnr.A2980

Table 1: Specific imaging parameters of the 4 individual DWI scans

Parameter	TR	TE	In-plane Spatial Resolution (mm^2)	Average Imaging Time (seconds)
128 × 128, R = 1[a]	8500.0	70.1-81.7	1.88	34
128 × 128, R = 3	3000.0	57.0-60.4	1.88	45
192 × 192, R = 1	8500.0	82.8-82.9	1.25	43
192 × 192, R = 3	3000.0	57.3-60.4	1.25	45

[a] Product sequence/routine protocol

institutional review board and was Health Insurance Portability and Accountability Act–compliant.

Patient Population

Patients were included on the basis of their ability to undergo MR imaging. Informed consent was obtained from each patient or the designated next of kin. Consecutive patients who met these criteria between January 2007 and August 2009 were included. All patients underwent the research DWI sequences as part of a clinically indicated MR imaging study used to evaluate stroke. Forty-eight patients met the inclusion criteria. Mean age was 66 years (range, 30–91 years) at the time of imaging, with slight male predominance (26 men, 22 women). On the basis of the reference standard readings, these patients were separated into the following groups: acute ischemic stroke ($n = 30$), ischemic stroke with hemorrhagic transformation ($n = 4$), intraparenchymal hemorrhage ($n = 9$), and no acute pathology ($n = 5$). Thirty-four of 48 patient scans contained diffusion-positive lesions based on the reference standard reading. The On-line Table presents the demographics of this group in more detail.

Imaging Protocol

DWI sequences with 4 different parameter settings were acquired in random order, at the same imaging session and at the same section locations on a 1.5T scanner (Signa; GE Healthcare, Milwaukee, Wisconsin). The different acquisition matrices and reduction factors were as follows: 1) 128 × 128 matrix (1.88 mm^2 in-plane resolution), R = 1; 2) 128 × 128 matrix and R = 3; 3) 192 × 192 matrix (1.25 mm^2 in-plane resolution) and R = 1; and 4) 192 × 192 matrix and R = 3. R is defined as the number of phase-encoding steps with PI relative to the number of phase-encoding steps without PI. The PI sequences were performed by using the GRAPPA technique, in which the GRAPPA kernel was derived and applied in hybrid space (ie, x-k_{PE}-space) as recently described.[13] Shared parameters for all scans included 5-mm section thickness with a 1.5-mm gap, $b = 0$ and 1000 s/mm^2 (tetrahedral encoding), and an FOV of 24 cm. Sequence TR depended on the total number of sections needed to cover the entire neurocranium and the EPI readout length (ie, acquisition matrix and reduction factor).

If one ignores geometry factor-based SNR influences with PI, the SNR decreases by the root ($\sqrt{}$) of the reduction factor. Because scan parameter settings were SNR-normalized, 3 averages were used to make up for the cube-root SNR loss for the R = 3 scans. This translated to slightly longer average scanning times for R = 3 scans, detailed in Table 1. However, the longer associated scanning time is not increased 3-fold because PI also shortens the EPI readout (proportional to the reduction factor), allowing additional sections to be acquired per TR. To minimize sequence TE, partial Fourier acquisition with 20 extra *k*-space lines was performed with subsequent homodyne reconstruction.[14] A tetrahedral encoding scheme was used,[15] and isotropic DWI and ADC maps were calculated by using standard techniques. Details of the different DWI scans are presented in Table 1. An 8-channel array coil was used (8HRBRAIN; GE Healthcare) for signal-intensity reception, whereas the body volume coil was used for signal-intensity excitation.

These 4 DWI sequences were incorporated into an overall neuroimaging protocol that varied on the basis of clinical presentation. All studies included at a minimum a 3-plane single-shot FSE T2-based localizer, an axial T2-weighted FSE, an axial gradient-echo, and an axial T2-weighted FLAIR sequence. Additional sequences variably included sagittal T1-weighted FSE; pregadolinium axial T1-weighted FSE; axial or 3-plane post-gadolinium-enhanced T1-weighted FSE; MR angiography and/or venography by using the 3D and 2D time-of-flight techniques, respectively; bolus 3D contrast-enhanced angiography of the neck; and axial EPI-based gadolinium bolus PWI sequences. These were not evaluated by the blinded reviewers but were available for use by another neuroradiologist (J.B.A.) to determine the most likely etiology of the patient's symptoms ("reference standard interpretation," see below).

Image Analysis

Diffusion images (isotropic DWI, $b = 0$, and trace ADC maps) for each set of DWI parameters were presented separately and in random order to 3 fellowship-trained academic neuroradiologists. All images were zero-filled to a 256 × 256 matrix, and patient identification and imaging-parameter information were removed from the images. The 4 DWI scans for each patient and the individual patients themselves were presented in a randomized fashion to avoid a memory effect and possible bias.

The readers were blinded to all patient identifiers, clinical presentation, symptoms, and imaging parameters. They rated each of the 4 DWI sequences (4 per patient for 48 patients, yielding 192 total DWI scans) on several image-quality metrics, including overall image quality, susceptibility artifacts, motion artifacts, subjective spatial resolution, subjective noise assessment, and subjective lesion conspicuity by using an ordinal 5-point Likert scale: 1 = much worse, 2 = worse, 3 = comparable with a typical DWI scan, 4 = better, and 5 = much better. For each rating, readers also selected their most likely diagnosis (ischemic stroke, ischemic stroke with hemorrhagic transformation, hemorrhage, or no lesion/no acute pathology) and stated their clinical confidence on a scale of 1–5 (1 = extremely unlikely, 2 = unlikely, 3 = equally likely and unlikely, 4 = likely, 5 = extremely likely). Readers also selected the vascular territory of a lesion, if ≥1 lesion was present. Finally, in cases in which lesions were present, readers were asked to specify whether those lesions were unilateral (left- or right-sided) or bilateral.

All images for each patient (including those additional sequences previously unavailable to the blinded readers, as well as the 4 DWI scans) were subsequently reviewed by another neuroradiologist (J.B.A., with 2 years of neuroradiology experience following American Board of Radiology certification) and were correlated with the clinical presentation, information available in the patient charts including discharge summary, and any pertinent available follow-up imaging. These data were then evaluated, with consideration of all available imaging and clinical information, and a final diagnosis was rendered as the reference standard interpretation for each patient. The reference standard interpretation was never in disagreement with the interpretations of at least 2 of the 3 expert readers for this study.

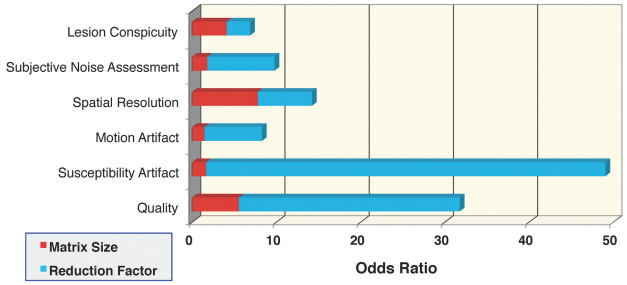

Fig 1. Graphic results of mixed-effects logistic regression with fixed factors of matrix size (128 or 192) and reduction factor (1 or 3). The odds ratio represents the odds that one will obtain a score of 4–5 (better than that of a standard DWI sequence) versus a score of 1–3 (equal to or worse than that of a standard DWI sequence).

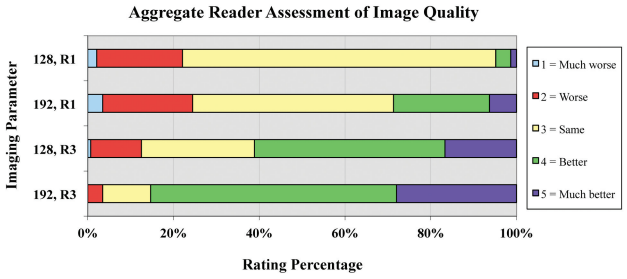

Fig 2. Effect of matrix size and reduction factor on reader assessment of overall image quality. (128, R1 = matrix size of 128 × 128, and reduction factor of 1.) Nominal values of 1–5 represent reader grading and assessment of image quality compared with the standard DWI SS–EPI phase-encoding scheme at 1.5T, represented by the percentage of total assigned values.

Statistical Analysis

A biostatistician (J.R.) performed all statistical analyses by using Stata, Release 9.2, software (StataCorp, College Station, Texas). Inter-rater agreement was first assessed by a linearly weighted κ to verify at least moderate agreement ($\kappa > 0.3$). Because the ratings were ordinal and not suitable for continuous regression analysis, they were dichotomized as either better or much better than a typical scan (rating scores = 4 and 5, respectively) or the same as, worse, or much worse than a typical scan (rating scores = 3, 2, and 1, respectively). The dichotomized values were then analyzed with a mixed-effects logistic regression with fixed factors of matrix size (128 or 192) and reduction factor (1 or 3) and random effects of patient and reader. The resulting odds ratios thus reflect the odds that a reader would evaluate an image as better than a typical image, rather than the same or worse.

Results

Odds ratios for ratings of DWI scans interpreted as better or much better than typical (scores = 4–5) are presented in Fig 1. Reduction factor (R = 3) had the greatest effect on susceptibility artifacts and overall image quality, with odds ratios of 47 ± 16, and 26 ± 7, and was preferred across all metrics. Lesion conspicuity was not decreased on the R = 3 images despite reductions in TE (and therefore a reduced T2 shine-through effect). Higher resolution was also preferred, regardless of whether parallel imaging was used, but to a lesser extent. Most interesting, subjective noise assessment, motion and susceptibility artifacts, and overall image quality appear to be most affected by reduction factor, whereas matrix size imparts a slightly greater contribution in perceived lesion conspicuity and, not surprisingly, perceived spatial resolution.

Table 2: Detailed statistical results of mixed-effects logistic regression with fixed factors of matrix size (128 or 192) and reduction factor (1 or 3)

	Parameter	Odds Ratio[a]	Std. Error	*Z*	95% CI
Lesion conspicuity	Matrix	4.083	1.035	5.55	2.484–6.712
	R	2.772	0.678	4.17	1.716–4.477
Noise assessment	Matrix	1.781	0.423	2.43	1.118–2.838
	R	7.980	2.320	7.14	4.513–14.108
Spatial resolution	Matrix	7.775	1.710	9.32	5.052–11.966
	R	6.424	1.403	8.52	4.187–9.857
Motion artifact	Matrix	1.435	0.461	1.12	0.764–2.695
	R	6.819	2.888	4.53	2.973–15.639
Susceptibility artifact	Matrix	1.645	0.412	1.99	1.007–2.687
	R	47.398	15.623	11.71	24.842–90.434
Quality	Matrix	5.526	1.384	6.83	3.382–9.028
	R	26.224	7.263	11.8	15.239–45.127

Note:—R indicates reduction factor.
[a] The odds ratio represents the odds that one will obtain a score of 4–5 (better than a standard DWI sequence) versus a score of 1–3 (equal to or worse than a standard DWI sequence).

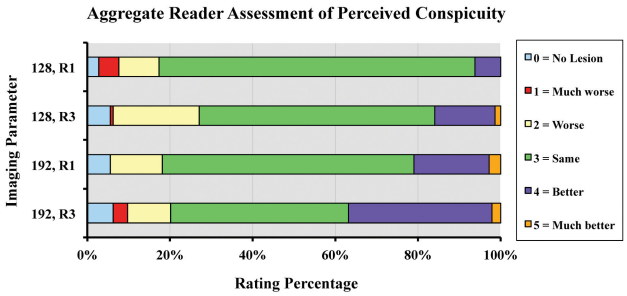

Fig 3. Effect of matrix size and reduction factor on reader assessment of lesion conspicuity. (128, R1 = matrix size of 128 × 128, and reduction factor of 1.) Nominal values 1–5 represent reader grading and assessment of lesion conspicuity compared with the standard DWI SS–EPI phase-encoding scheme at 1.5T, represented by the percentage of total assigned values.

The effect of matrix size and reduction factor on reader assessment of overall image quality is shown in Fig 2 and Table 2. Additional effects of matrix size and reduction factor on reader assessment of perceived spatial resolution, susceptibility artifacts, motion artifacts, and noise are depicted in On-line Figs 1–4. The 128 × 128 matrix, R = 1 DWI images (equivalent to our standard or routine DWI at 1.5 T) received the greatest percentage of ratings of 3 in assessing image quality (73% of cases), indicating that readers generally recognized this scan as being equivalent to that of standard SS–EPI DWI. The 192 × 192, matrix R = 3 sequence received the greatest percentage of 4 and 5 scores, denoting improved image quality (85% of cases). Finally, the 192 × 192, matrix R = 3 sequence was the only 1 of the 4 sequences that did not to receive a score of 1 (much worse) by any reader.

The results of subjective lesion conspicuity are presented in Fig 3 and show that both improved spatial resolution and reduction factor result in more conspicuous lesions. The number of "no lesion" tallies per technique increased with spatial resolution and reduction factor, suggesting that there is a decreased incidence of distortion-related artifacts that are misconstrued as true DWI-positive lesions; this finding was also supported by the reference standard final readings.

DWI scans with different spatial resolution and reduction factors are depicted in Figs 4 and 5, highlighting how differ-

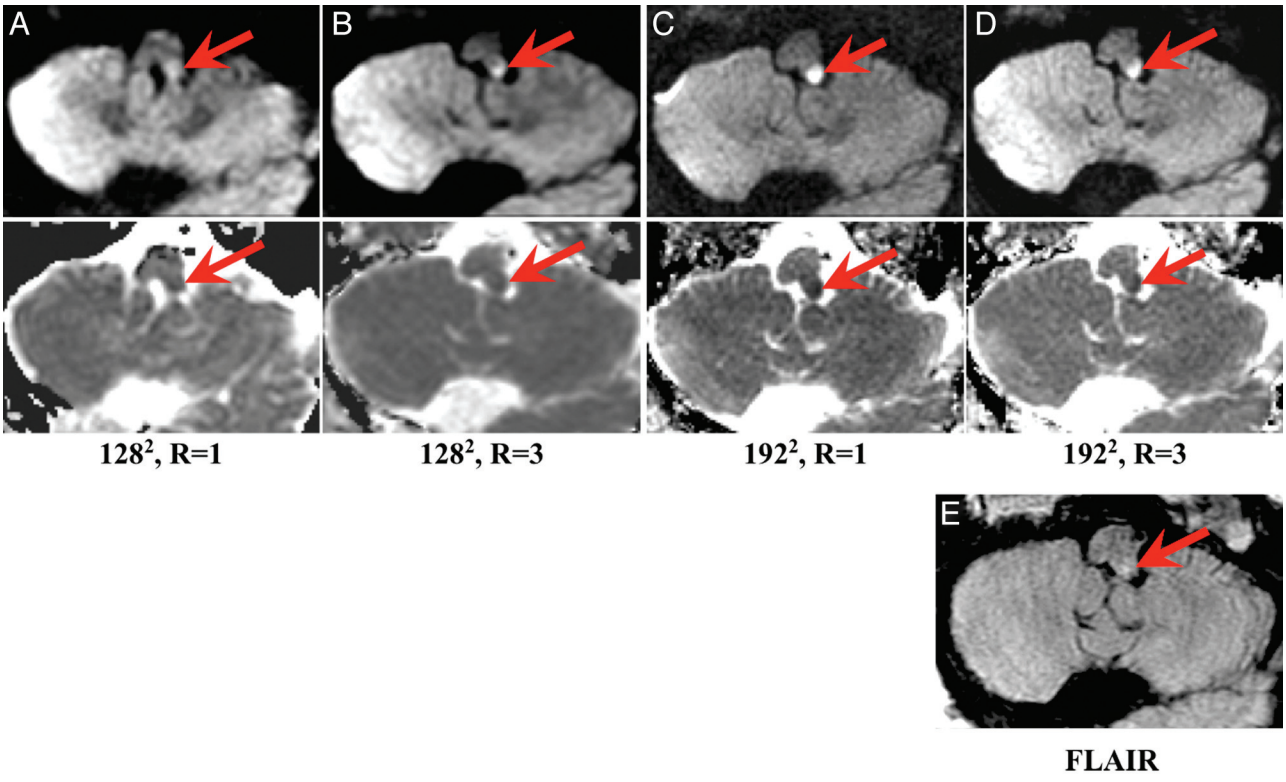

Fig 4. MR images of an 82-year-old patient with new onset of diplopia, who was found to have a left dorsolateral medullary infarct (*red arrow*) as depicted on representative diffusion images (upper row) and the corresponding ADC map (lower row) with matrix size and reduction factor as follows: *A*, 128^2, R = 1; *B*, 128^2, R = 3; *C*, 192^2 R = 1; *D*, 192^2 R = 3. Corresponding FLAIR image (*E*) demonstrates minimal associated edema suggesting acute onset. One of 3 readers graded the 128^2, R = 1 and 128^2, R = 3 scans as having "no lesion" but correctly graded the higher matrix size scans (192^2, R = 1 and R = 3) as infarct, highlighting the increased conspicuity of the lesion by using a higher matrix size. The 2 remaining readers correctly graded this lesion for all presented imaging parameters.

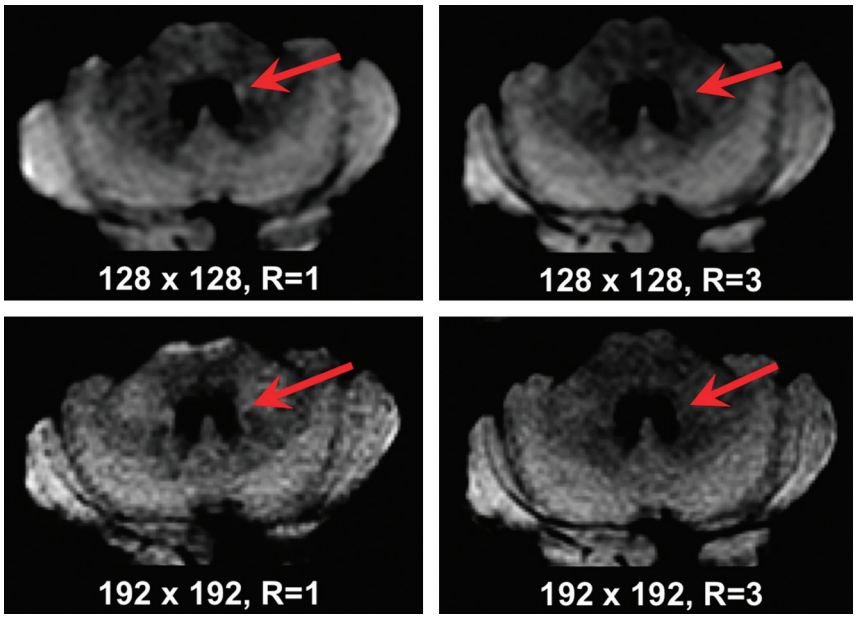

Fig 5. Diffusion images in a 70-year-old patient with right-sided numbness: Small acute left thalamic infarct (not shown) and tiny presumed left middle cerebellar peduncular infarct identified on the matrix = 128^2, R = 1 image (*red arrow, upper left figure*), determined to be artifacts on other DWI images (*upper right figure*, 128^2, R = 3; *lower left figure. C*, 192^2, R = 1; *lower right figure. D*, 192^2, R = 3) and standard MR images (not shown), altering the diagnosis from thromboembolic to lacunar infarct in 2 of 3 readers (2 of 12 DWI scan interpretations).

ences in technique affect the perceived presence of acute/early subacute infarcts. Figure 4 provides an example of the role that parallel imaging and increased matrix size may play in increasing lesion conspicuity and, thereby, lesion detection. Figure 5 provides an example in which parallel imaging and higher matrix size help to distinguish a diffusion-positive lesion (based on 2 expert reader interpretations) from artifacts. Figure 6 illustrates how parallel imaging may assist in identifying addi-

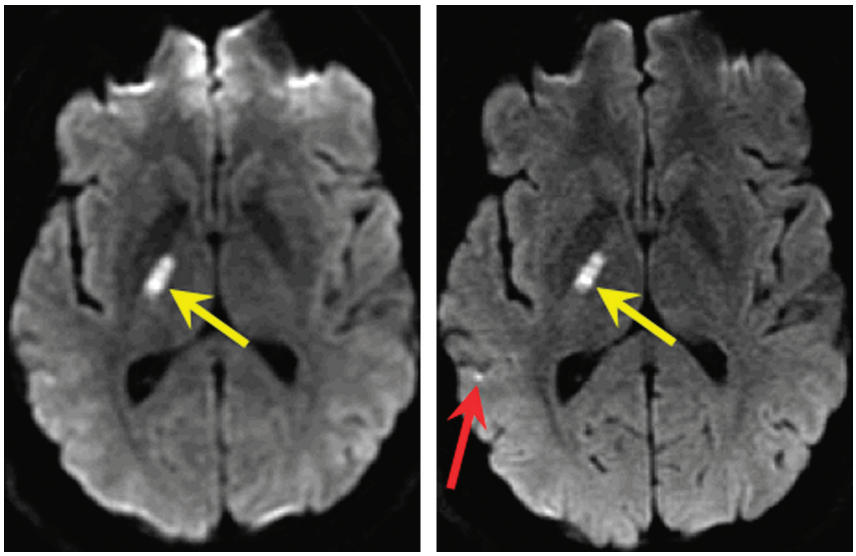

Fig 6. Diffusion images in a 48-year-old man with left-sided hemiparesis. The image on the left was obtained using matrix = 128^2, R = 1, while the image on the right was obtained using matrix = 192^2, R = 3. The right basal ganglia infarct (*yellow arrow*) is conspicuous on both images. However, the right temporal lobe punctate focus of diffusion signal-intensity abnormality (red arrow) is more conspicuous when imaged with higher reduction factor and matrix size (image on the right). This second infarct, in a superficial-versus-deep MCA territory, led to a search for an extracranial source.

tional lesions that might otherwise be overlooked by using more traditional SS–EPI readout schemes.

Discussion

DWI has become the cornerstone of acute stroke imaging. Given the reliance on MR imaging in the work-up of stroke and its mimics and the prevalence of 1.5T MR imaging systems, it is imperative that DWI be fully optimized to allow immediate and correct diagnosis. While earlier studies performed at 3T have indicated that parallel imaging (by using the sensitivity encoding technique) might improve the diagnostic quality of DWI,[9,12,16] whether higher spatial resolution or PI reduction factors individually or conjointly impact the diagnosis of stroke at 1.5T thus far has not been investigated, to our knowledge.

The R = 3 scans demonstrated improvement in overall image quality, including reduction in geometric distortion, subjective noise assessment, and motion degradation, and were preferred across all metrics. Lesion conspicuity and spatial resolution were most affected by changes in spatial resolution rather than reduction factor, though both imaging characteristics were affected by both parameters. This is due, most likely, to a more pronounced effect of matrix size on TE than that of R and the associated stronger T2 shine-through effect in the patient population studied. Eighty-five percent of 192 × 192, R = 3 images received ratings of "better" or "much better" than standard DWI. Only 4% of 192 × 192, R = 3 images received a rating of 2 ("worse" than standard), partially attributable to increased patient motion. A rating of 1 was not assigned to any scan with these imaging parameters. In short, the 192 × 192, R = 3 images were rated equal to or superior to the current standard in 96% of cases.

The clinical relevance of these preferences remains unclear, because standard DWI parameters (128 × 128 matrix, R = 1) at 1.5T allowed visualization of most of the lesions present in this study. Overall, improved image quality did not result in changes in the assignation of underlying stroke etiology. There were, however, 5 individual examples (2 of which are illustrated in Figs 1 and 2) in which there was a change in diagnosis with the use of altered imaging parameters (192 × 192 matrix, R = 3), suggesting that the use of higher spatial resolution and reduction factor improves diagnostic accuracy. Furthermore, in situations in which there was no change in diagnosis with the use of the nonstandard DWI sequences, there was still a statistically significant increase in diagnostic confidence, particularly for the 192 × 192 matrix, R = 3 sequence. This observation is in accordance with previously reported findings using PI in the evaluation of stroke.[16,17] Higher spatial resolution and/or reduction factor led to correct identification of these lesions (based on the reference standard reading), altered the diagnosis in 5 patients (up to 10% per expert reader) with posterior circulation acute ischemic stroke, and altered the diagnosis from small-vessel to cardioembolic stroke in 2 patients due to identification of lesions in separate vascular territories (up to 5% change per reader). These findings suggest that the benefits of imaging with higher spatial resolution and reduction factor are tangible and result in clinically relevant changes in patient management and potential patient outcome.

In this study, supratentorial lesions were more likely to be correctly identified regardless of imaging parameters used while those in the posterior fossa, notably in the vertebrobasilar distribution, were more likely to go undetected on scans obtained at a lower matrix size and reduction factor. Specifically, the locations where lesions were most likely to go unnoticed were those involving the medulla and, to a lesser extent, the pons and middle cerebral peduncles. This is likely secondary to the susceptibility and geometric distortion effects commonly encountered in the posterior fossa and near the skull base on routine DWI. Alternatively, the small size of the interrogated structures and relative absence of more distinct anatomic lateralization in this region may highlight the improvements of spatial resolution and reduced geometric distortion.

Evaluation of subjective lesion conspicuity, illustrated in Fig 1 and Table 2, is complicated by the subjective nature of

initial lesion detection, followed by the subjective assessment of how conspicuous a lesion was perceived to have been on detection. This is further confounded by the observation that the conspicuity of missed lesions cannot be assessed (ie, a lesion that was not detected cannot be evaluated). There is a suggestion that increasing matrix size and reduction factor decreases the number of false-positive evaluations as a result of a decreased incidence of geometric-distortion-related artifacts, which, in a small proportion of patient scans, were misconstrued as DWI-positive lesions when imaged at 128 × 128, R = 1. A larger sample size would be beneficial to further evaluate this phenomenon.

One of the initial working hypotheses of this study was that because PI reduces geometric distortions and enhances image quality, additional lesions in additional vascular territories might be found, in turn suggesting a different underlying stroke etiology (ie, embolic versus lacunar). While improved image quality and improved lesion conspicuity were demonstrated by using the R= 3 higher-resolution technique, instead of seeing more lesions, we found that higher resolution and reduction factors were more likely to result in correct interpretation of equivocal lesions as artifacts. In cases in which additional lesions were seen, they were typically in the same vascular territory and did not alter the mechanism of injury. A larger study population might, however, allow us to realize additional lesions that could support an embolic over a lacunar or watershed mechanism. Furthermore, a larger study might allow better characterization of the effect that the reduction factor has on lesion conspicuity relative to matrix size, which appears to be less significant in the current study compared with the other evaluated imaging-quality metrics.

Limitations of this study include the lack of a predefined diffusion-negative cohort (such as healthy subjects). Additionally, only 4 distinct sets of imaging parameters were evaluated so as not to increase unduly the length of these clinical MR imaging studies. We also did not attempt to set the TE values to a standard to remove the effects of T2 shine through but rather concentrated on the shortest TEs possible for each imaging parameter combination, because this is very likely how such sequences would be implemented in the clinical setting to maximize the signal intensity to noise of the examination. Finally, our definition of the "reference standard" read may be deemed a problematic standard of reference. The "reference standard" diagnosis was, however, determined only after image interpretation and correlation with all available patient data were reviewed. Moreover, in no case in this study did the "reference-standard" differ from the interpretation of at least 2 readers when evaluated over all 4 DWI scans per patient.

Conclusions

Our study suggests that PI benefits diffusion imaging at 1.5T and that most of this benefit comes from the reduced geometric distortion associated with higher reduction factors and, to a lesser degree, from higher spatial resolution. PI did not have any adverse effects on lesion conspicuity, subjective noise assessment, or motion artifacts, similar to findings in previous reported studies evaluating PI. In situations in which PI cannot be implemented (lack of hardware, software, or appropriate coils), higher spatial resolution (192 × 192 versus 128 × 128) may improve DWI. Of the 4 imaging conditions studied, we found that 192 × 192 matrix, R = 3 offered the best imaging conditions for clinical DWI at 1.5T and was preferred over either independently adjusted higher resolution or higher reduction factors. As a result, these parameters (192 × 192 matrix, R = 3) are now used for all clinical stroke MR imaging at the authors' institution (Stanford University Medical Center). Moreover, the results suggest that the slightly longer imaging time needed to acquire images of comparable signal intensity to noise is justified, when using PI and higher reduction factors.

Disclosures: Greg Zaharchuk—*UNRELATED: Consultancy:* GE Healthcare, *Comments*: Neuroradiology Advisory Board, *Grants/Grants Pending*: Multiple NIH Grants. Nancy J. Fischbein—*RELATED: Grant*: NIH,* *Comments*: Grant support to Roland Bammer, and a small percentage to me, for our GRAPPA development work, *UNRELATED: Board Membership*: *American Journal of Neuroradiology* Senior Editor. Maarten G. Lansberg—*RELATED: Grant*: NIH.* Stephanie Kemp—*RELATED: Grant*: NIH,* *UNRELATED: Grants/Grants Pending*: NIH.* Greg W. Albers—*UNRELATED: Consultancy*: Lundbeck, *Grants/Grants Pending*: NIH.* Roland Bammer—*RELATED: Grant*: NIH;* *UNRELATED: Grants/Grants Pending*: NIH.* *Money paid to the institution.

References

1. Moseley ME, Wendland MF, Kucharczyk J. **Magnetic resonance imaging of diffusion and perfusion.** *Top Magn Reson Imaging* 1991;3:50–67
2. Lutsep HL, Albers GW, DeCrespigny A, et al. **Clinical utility of diffusion-weighted magnetic resonance imaging in the assessment of ischemic stroke.** *Ann Neurol* 1997;41:574–80
3. Lansberg MG, Thijs VN, Hamilton S, et al. **Evaluation of the clinical-diffusion and perfusion-diffusion mismatch models in DEFUSE.** *Stroke* 2007;38:1826–30
4. Easton JD, Saver JL, Albers GW, et al, for the American Heart Association; American Stroke Association Stroke Council; Council on Cardiovascular Surgery and Anesthesia; Council on Cardiovascular Radiology and Intervention; Council on Cardiovascular Nursing; Interdisciplinary Council on Peripheral Vascular Disease. **Definition and evaluation of transient ischemic attack: a scientific statement for healthcare professionals from the American Heart Association/American Stroke Association Stroke Council; Council on Cardiovascular Surgery and Anesthesia; Council on Cardiovascular Radiology and Intervention; Council on Cardiovascular Nursing; and the Interdisciplinary Council on Peripheral Vascular Disease. The American Academy of Neurology affirms the value of this statement as an educational tool for neurologists.** *Stroke* 2009;40:2276–93. Epub 2009 May 7
5. Purroy F, Begue R, Gil MI, et al. **Patterns of diffusion-weighted magnetic resonance imaging associated with etiology improve the accuracy of prognosis after transient ischaemic attack.** *Eur J Neurol* 2011;18:121–28
6. Moseley ME, Kucharczyk J, Mintorovitch J, et al. **Diffusion-weighted MR imaging of acute stroke: correlation with T2-weighted and magnetic susceptibility-enhanced MR imaging in cats.** *AJNR Am J Neuroradiol* 1990;11:423–39
7. Bammer R, Keeling SL, Augustin M, et al. **Improved diffusion-weighted single-shot echo-planar imaging (EPI) in stroke using sensitivity encoding (SENSE).** *Magn Reson Med* 2001;46:548–54
8. Pruessmann KP, Weiger M, Scheidegger MB, et al. **SENSE: sensitivity encoding for fast MRI.** *Magn Reson Med* 1999;42:952–62
9. Griswold MA, Jakob PM, Heidemann RM, et al. **Generalized autocalibrating partially parallel acquisitions (GRAPPA).** *Magn Reson Med* 2002;47:1202–10
10. Ra JB, Rim CY. **Fast imaging using subencoding data sets from multiple detectors.** *Magn Reson Med* 1993;30:142–45
11. Sodickson DK. **Tailored SMASH image reconstructions for robust in vivo parallel MR imaging.** *Magn Reson Med* 2000;44:243–51
12. Skare S, Newbould RD, Clayton DB, et al. **Clinical multishot DW-EPI through parallel imaging with considerations of susceptibility, motion, and noise.** *Magn Reson Med* 2007;57: 881–90
13. Brau AC, Beatty PJ, Skare S, et al. **Comparison of reconstruction accuracy and efficiency among autocalibrating data-driven parallel imaging methods.** *Magn Reson Med* 2008;59:382–95
14. Noll DC, Nishimura DG, Macovski A. **Homodyne detection in magnetic-resonance-imaging.** *IEEE Trans Med Imaging* 1991;10:154–163
15. Conturo TE, McKinstry RC, Akbudak E, et al. **Encoding of anisotropic diffusion with tetrahedral gradients: a general mathematical diffusion formalism and experimental results.** *Magn Reson Med* 1996;35:399–412
16. Kuhl CK, Gieseke J, von Falkenhausen M, et al. **Sensitivity encoding for diffusion-weighted MR imaging at 3.0 T: intraindividual comparative study.** *Radiology* 2005;234:517–26
17. Holdsworth SJ, Yeom K, Skare S, et al. **Clinical application of readout-segmented-echo-planar imaging for diffusion-weighted imaging in pediatric brain.** *AJNR Am J Neuroradiol* 2011;32:1274–79